Jurnal Teknologi

Full paper

Effect of Velocity Variation at High Swirl on Axial Flow Development inside a Can Combustor

Mohamad Shaiful Ashrul Ishak[a,b*], Mohammad Nazri Mohd. Jaafar[b]

[a]School of Manufacturing Engineering, Universiti Malaysia Perlis, P.O Box 77, Pejabat Pos Besar, 01000 Kangar, Perlis, Malaysia
[b]Department of Aeronautics, Automotive & Ocean Engineering, Faculty of Mechanical Engineering, Universiti Teknologi Malaysia, 81310 UTM, Universiti Teknologi Malaysia, 81310 UTM Johor Bahru, Johor Malaysia

*Corresponding author: mshaiful@unimap.edu.my

Article history

Received 2 April 2014
Received in revised form 24 June 2014
Accepted 24 August 2014

Graphical abstract

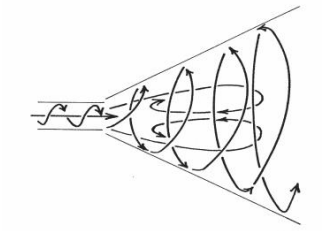

Abstract

The main purpose of this paper is to study the internal flow effect of varying the inlet velocities inside a combustor. The flow field inside the combustor is controlled by the liner shape and size, wall side holes shape, size and arrangement (primary, secondary and dilution holes), and primary air swirler configuration. Air swirler adds sufficient swirling to the inlet flow to generate central recirculation region (CRZ) which is necessary for flame stability and fuel air mixing enhancement. Therefore, designing an appropriate air swirler is a challenge to produce stable, efficient and low emission combustion with low pressure losses. Four various injection velocities from 30m/s to 60m/s with radial vanes angle of 50 degree were used in this analysis to show velocity effect on the internal flow field. The flow behavior was investigated numerically using CFD solver Ansys 14.0. This study has provided the characteristic insight into the flow pattern inside the combustion chamber. Results show that the swirling action is augmented with the increase in the injection velocity, which leads to increase in core reverse flow, thus enhancing mixing of fuel and air in the combustion chamber.

Keywords: Swirler; swirl number; combustor; turbulence; CFD simulation

1.0 INTRODUCTION

Swirling jets are used for the stabilisation and control of a flame to achieve a high intensity of combustion. The common method of generating swirl is by using angle vanes in the passages of air. The characteristic of the swirling jet depends on the swirler vane angle [1]. Various investigation on the effects of swirl on the flame stability for swirl flame in the unconfined space have shown increasing fuel/air mixing as the degree of swirl increased [2,3]. The size and strength of the central recirculation zone (CRZ) also increased with an increase in swirl intensity. At low flow rates or swirl number, a long yellow and highly luminous flames in produced indicating a poor mixing [3]. However, when the swirl number is increased, the CRZ increases in size, initially in width until restricted by diameter of combustor and then begin to increase in length [3]. Measurements of the flame length and stabilization distance carried out in the series of butane/air and propane/air flames with swirl have shown that both decrease markedly with increasing degree of swirl [4]. Increasing of swirl number improves the flame stability due to the presence of the recirculation zone [5]. Increasing the swirl number increase the angle of jets thereby increasing the total available surface area per unit volume of the jet for mixing with the surrounding fluid in free jet and enclosure jet diameter ratio [6]. It has been shown that flames with low swirl have instability problems, because of the absence of the recirculation zone [7].

As shown schematically in Figure 1, jet flow of high degree of swirl often results in significant lateral as well as longitudinal pressure gradients. Compared to its non-swirling counterpart, the jet is much wider, slower and with a central toroidal recirculation zone. In combustion, the presence of the recirculation zone plays important role in flame stabilization by providing a hot flow of recirculated combustion products and a reduced velocity region where flame speed and flow velocity can be matched. Swirls also act to shorten the flame length and this is advantageous for having more compact burner design [8].

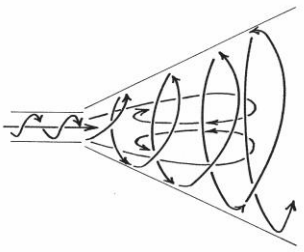

Figure 1 Jet flow of high degree of swirl (S > 0.6) resulting in significant lateral as well as longitudinal pressure gradients. Compared to its non-swirling counterpart, the jet is much wider, slower and there exist a central toroidal recirculation zone [8]

The geometric swirl number (S_N) has been formulated by Al-Kabie [9] and given as;

$$S_N = \frac{\sin\theta}{1+1/\tan\theta}\left[\frac{A_a}{C_c A_{th}}\right] \quad (1)$$

where

A_a is the swirler exit area
A_{th} is the swirler minimum throat area
C_C is the swirler contraction coefficient

Value for C_C, the swirler contraction coefficient, C_D, the swirler discharge coefficient and hence the swirl number was obtained using the following Equation (2) and Equation (3). The discharge coefficient in term of swirler pressure drop and air mass flow rates can be obtained as;

$$C_D = \frac{\dot{m}}{A_{th}\sqrt{2\rho\Delta P}} \quad (2)$$

Where

$\dot{m}$ is the volumetric air flow rates
ΔP is the pressure drop

An expression for contraction coefficient in term discharge coefficient, throat area and swirler exit area can be obtained as follow;

$$C_C = \frac{C_D}{1+\left(\frac{C_D A_{th}}{A_a}\right)} \quad (3)$$

The swirl number should, if possible, be determined from measured values of velocity and static pressure profiles. However, this is frequently not possible due to the lack of detailed experimental results. Therefore, it has been shown that the swirl number may be satisfactorily calculated from geometry of most swirl generator [10].

The main focus of this research is to investigate the effect of inlet velocity to the swirling flow inside the combustor. Flow pattern characteristics include velocity components and turbulent stresses, which are the main characteristics of the swirling flows, have been studied to understand the physical process both by numerical modeling CFD software Ansys 14.0 [11].

■2.0 MODELING, MESHING AND BOUNDARY CONDITION

The basic geometry of the gas turbine can combustor is shown in Figure 2 and Figure 3. The size of the combustor is 1000 mm in the length and 280mm inner diameter. The primary inlet air is guided by radial curve vanes swirler to give the air a swirling velocity component. The transverse analysis is focused downstream of the swirler in the expansion chamber at various cross section stations (z/D = 0.2 to 1.0) as shown in Figure 3.High swirl number of swirler with vane angle of 50° were analyzed numerically at different velocity inlet (u) ranging from 30 to 60 m/s (Reynolds Number from 0.6 to 1.2 x 10^6) conditions to show the effect of the air inlet on the turbulence production, recirculation zone and also pressure loss. The technical data of the swirler used in this study are listed in Table 1. The attributes associated with mesh quality are node point distribution, smoothness, and skewness. Therefore, in order to generate an accurate solution with less computation effort, smaller hexahedral-type mesh elements 10^{-9} m^3 volume were used in the region of interest, i.e. at high gradient zones where the main flow expands from the swirler jet and where recirculation zone was located. Mesh growth rate was taken in range of 1% to 2% to guarantee smoothness and low aspect ratio meshes and the maximum volume allowed was 3.4 x 10^{-6} m^3. The combustor model meshing for the present work is shown in Figure 4.

Due the complexity of the flow within the gas turbine combustor, CFD is used as a regular tool to enable better understanding of the aerodynamic and process associated with combustion inside the gas turbine combustors. As mentioned above, FLUENT solves the equations for conservation of mass and momentum in their time averaged form for the prediction of isothermal flow fields. For the process of Reynolds decomposition and time averaging results in unknown correlation of the fluctuation velocity components, a turbulence model is required for equations closure purposes. In the present simulation, k-epsilon turbulence model was used. Turbulence is represented by the realizable k-epsilon model, which provides an optimal choice and economy for many turbulent flows [12, 13]. This work had studied the behavior of five k-epsilon variants in modelling the isothermal flow inside a gas turbine combustor and compared the results with the experimental data of Da Palma [14] for the velocity and turbulence fields. The studied models were the standard, the RNG, the realizable, the Durbin modified, and the nonlinear k-epsilon models. The results showed that the standard and the Durbin k-epsilon models gave the best agreement with the experimental data. This supported the finding of Durst and Wennerberg, where good agreement between k-epsilon model predictions and experimental results were reported [15]. This also agrees with Zhou et al. in their study on low NOx burner design [16].

The appropriate choice of boundary conditions is essential and is a critical part in modelling a flow accurately. Typical boundary conditions for FLUENT simulation are the inlet, the wall and the outlet boundaries. At the inlet of the computational region, the inlet boundary condition is defined as velocity inlet while the exit boundary is defined as outflow. Some assumptions for boundary conditions that were not directly measured had to be made as follows:

i. Velocity components and turbulence quantities at the inlet were constant,
ii. Turbulence at inlet is calculated from the following equations [17]:

$$k_{inlet} = 0.002(u^2)_{inlet} \quad (4)$$

$$e = \frac{k_{inlet}^{1.5}}{0.3D} \quad (5)$$

where u is axial inlet flow velocity and D is hydraulic diameter.

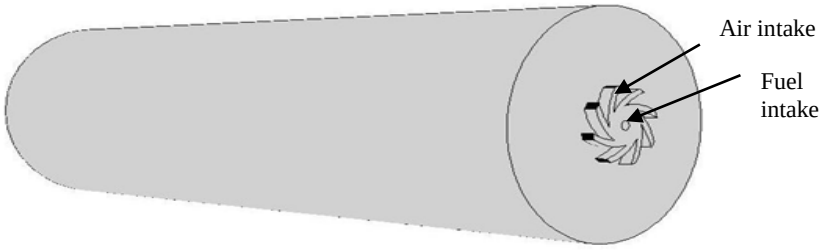

Figure 2 Combustor model

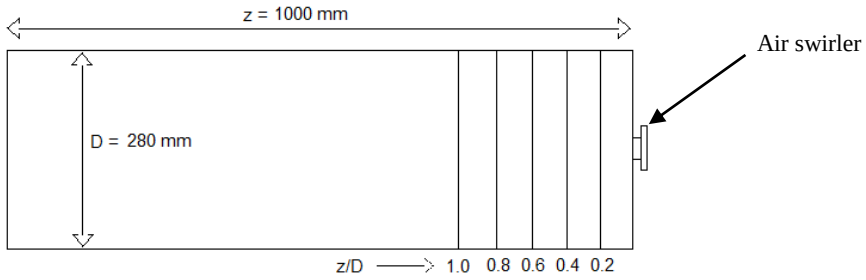

Figure 3 Details of position of transvers measuring stations indicated by cross section lines (z/D = 0.2 to 1.0) from the swirler throat

Table 1 Technical data of the swirlers

Swirler angle	50°
Calculated Swirl No. (S_N), Based on simulation	0.978
Passage width, *h* (mm)	11.2
Hub diameter, *d* (mm)	50
Outer diameter, *D* (mm)	98

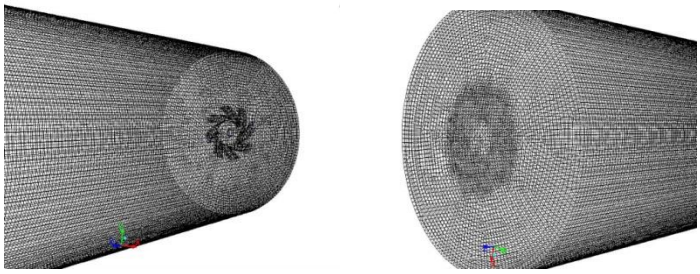

Figure 4 Combustor model meshing

3.0 DISCHARGE COEFFICIENT

In order to achieve better mixing between fuel and air in liquid fuel burner, turbulence flow must be generated to promote mixing. Turbulence energy is created from the pressure energy dissipated downstream of the flame stabilizer. In the radial swirler, turbulence can be generated by increasing the aerodynamic blockage or by increasing the pressure drop across the swirler. The discharge coefficient for radial swirler were obtained by passing an air flow through the radial swirler and flame tube while monitoring the static pressure loss upstream of the radial swirler relative to the atmospheric pressure. The results were plotted as a function of Reynolds number and presented in Figure 5. From Figure 5, it can be seen generally that all discharge coefficients were approximately constant with variation in Reynolds number. Thus the value of discharge coefficient may be concluded to be independent of Reynolds number. In the case of 50º vane angle swirler, the C_D is around 0.65.

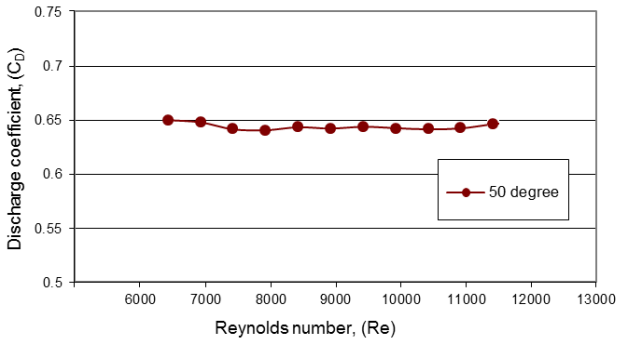

Figure 5 Discharge coefficient vs Reynolds number

4.0 RESULTS AND DISCUSSION

All the axial flow characteristics are presented in Figures 6 to 9. To validate the CFD model, experiments were conducted to measure the axial flow velocity at the axis of the chamber for 50 m/s inlet velocity. Figure 6 shows the results of CFD analysis compared to experimental results as part of the validation of the CFD model.

A past researcher shows that, 50° swirl gives the best result in terms of swirl zone and size of recirculation areas [18, 19, 20]. From the results, further work was conducted to see the effects of variations in axial velocity on the centre core flow in the combustion chamber. The flow was varied from 30 m/s to 60 m/s (equivalent to Reynolds Number from 0.6 to 1.2 x 10^6). The results showing the variations in the transient core flow at 25 s after the air was injected into the chamber are depicted in Figures 7. The figures show the reverse axial velocities in the central axial section of the chamber. The white portion of the figures means the axial flow is positive.

The results show similar flow pattern for all injection velocities, or at all Reynolds numbers, but as the injection velocities increased the reverse flow velocities in the core increases from 15 m/s for the 30 m/s injection (Figure 8a) to 30m/s for 60 m/s injection (Figure 8d). But the core size does not change. Taking the cross section at L/D= 0.1, the core size is r/R=0.05 for all injection velocities. The differences are mainly due to higher injection velocities, where the core reverse flow velocities also increases. These can be seen in the reverse axial velocities at different cross sections as shown in Figures 8a to 8d. Another significant result is that the core axial flow velocities at cross sections nearer to the injection point increases with injection speeds. But after the distance of L/D=0.4 the central core axial velocity does not change significantly. This can be seen clearly in Figure 7, and from Figures 8a to 8b.

The axial flow velocities along the central chamber axis were then plotted until 200 mm (L/D=0.71) from the injection point. In Figure 9, shows that near the injection point, the reverse flow velocities are directly related to the injection velocities. The higher the injection velocities, the faster are the reverse flow velocities. This is accompanied by the reduction in size of the core reverse flow volume. This is understandable since the swirl angle is constant (so is the swirl number), such that the higher injection velocities would produce higher reverse core flow, thus enhancing mixing of fuel in the chamber.

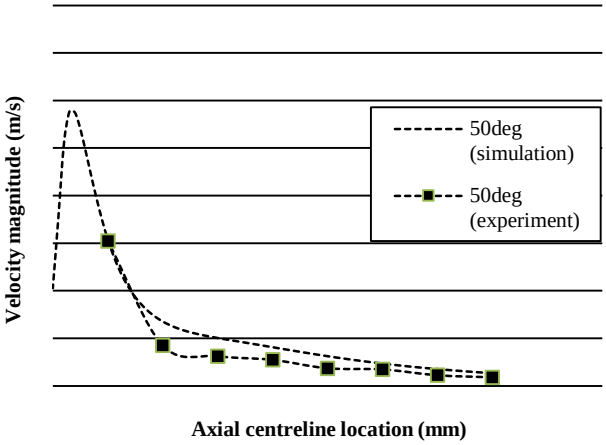

Figure 6 Axial Flow Velocity results from CFD Analysis for Combustors with 50° Swirl Angles, experiment with 50 m/s air inlet velocity

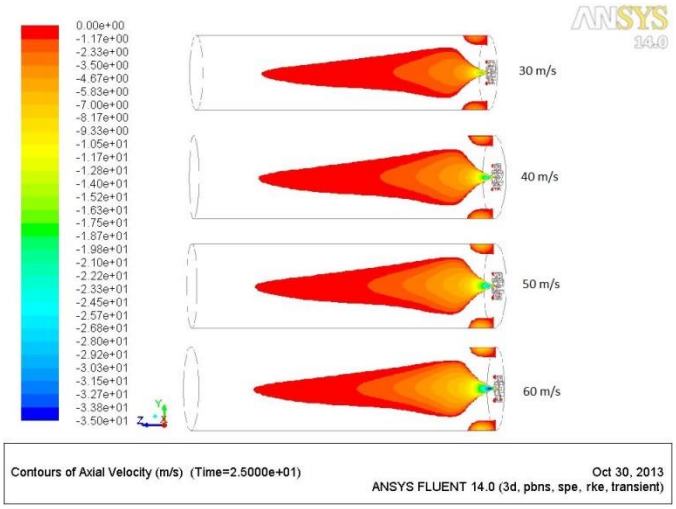

Figure 7 Transient flow at 25 s for varying injection velocities

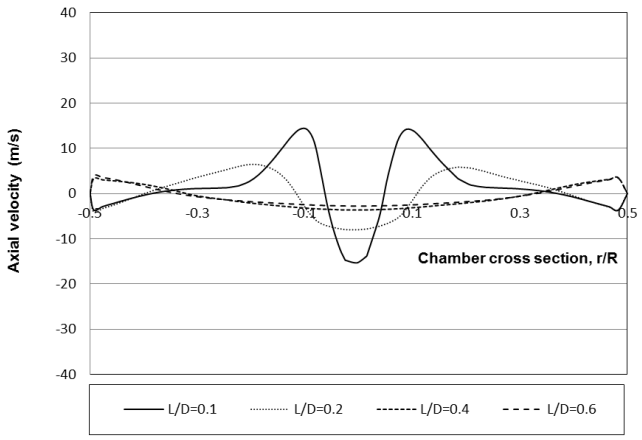

Figure 8a Axial flow across chamber diameter for injection velocity 30 m/s, at different cross section distances from the injection point

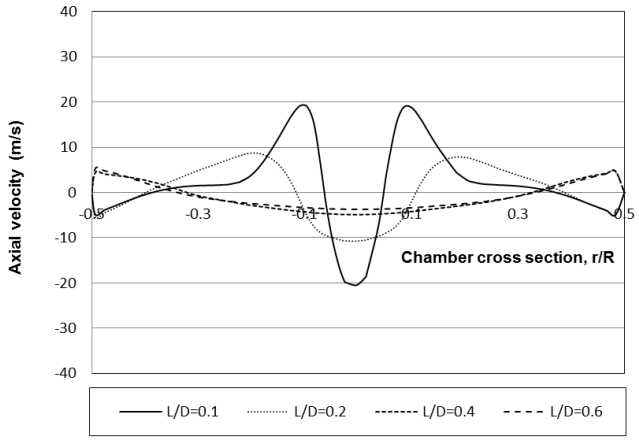

Figure 8b Axial flow across chamber diameter for injection velocity 40 m/s, at different cross section distances from the injection point

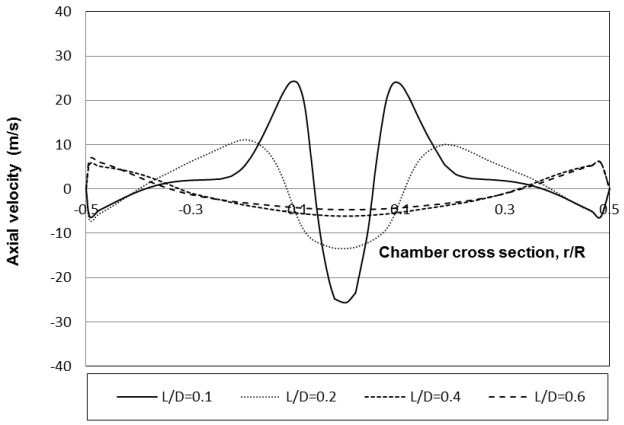

Figure 8c Axial flow across chamber diameter for injection velocity 50 m/s, at different cross section distances from the injection point

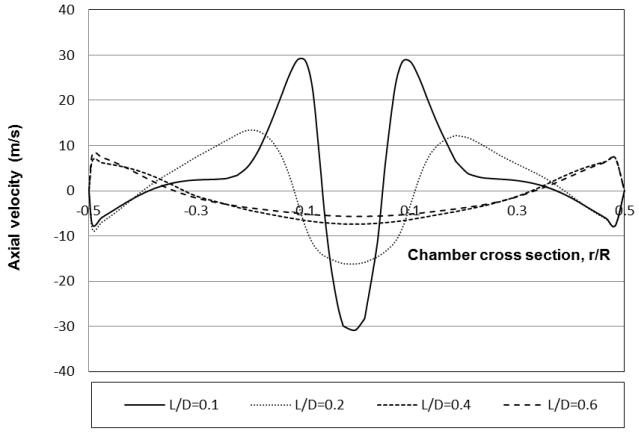

Figure 8d Axial flow across chamber diameter for injection velocity 60 m/s, at different cross section distances from the injection point

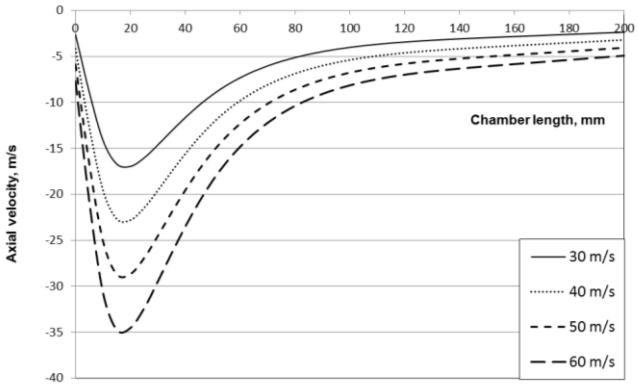

Figure 9 Axial flow along the velocities for different

5.0 CONCLUSION

This paper presented results of CFD study on the axial flow in a circular chamber with different inlet velocity vary from 30 m/s to 60 m/s (equivalent to Reynolds Number from 0.6 to 1.2 x 10^6) of 50 degree radial vane angle swirler. The initial results were compared with actual measurements to validate the CFD model. The validated model was then used to study further variations of the flow in the chamber. The study indicated that at all injection velocity, similar flow pattern was found, but as the injection velocities increased the reverse flow velocities in the core increase but the core size does not change. The differences are mainly due to higher injection velocities, where the core reverse flow velocities also increases. Another significant result is that the core axial flow velocities at cross sections nearer to the injection point increases with injection speeds. But after the distance of L/D=0.4 the central core axial velocity do not change significantly. From the results of various injection velocities, it shows that the differences are mainly due to higher injection velocities, where the core reverse flow velocities also increases.

Acknowledgement

The authors would like to thank the Ministry of Higher Education of Malaysia & Research Management Center (project number: 01G60) for awarding a research grant to undertake this project. The authors would also like to thank the Faculty of Mechanical Engineering, Universiti Teknologi Malaysia for providing the research facilities and space to undertake this work.

References

[1] D.L. Mathur. 1974. A New Design of Vanes for Swirl Generation. *IE (I) Journal ME*. 55: 93–96.
[2] N. Fricker and W. Leuckel. 1976. The Characteristic of Swirl Stabilized Natural Gas Flame Part 3: The Effect of Swirl and Burner Mouth Geometry on Flame Stability. *J. Inst. Fuel*. 49: 152–158.
[3] A. Mestre and A. Benoit. 1973. Combustion in Swirling Flow. *Proc. 14th Symposium (International) on Combustion, The Combustion Institute.* Pittsburgh. 719.
[4] A. Chervinskey and Y. Manheimertiment. 1968. Effect of Swirl on Flame Stabilization. *Israel Journal of Technology*. 6(2): 25–31.
[5] K. H. Khalil, F. M. El-Mehallawy and H. A. Moneib. 1977. Effect of Combustion Air Swirl on the Flow Pattern in a Cylindrical Oil Fired Furnace, *Proc. 16th Symposium (International) on Combustion, The Combustion Institute*, Pittsburgh. 135–143.
[6] G. Apack. 1974. *Interaction of Gaseous Multiple Swirling Flames*, Phd thesis, Department of Chemical Engineering and Fuel Technology, University of Sheffield.
[7] A.K. Gupta, D.G. Lilley and N. Syred. 1984. *Swirl Flows.* Abacus Press, Tunbridge Wells, England.

[8] R.H. Chen and J.F. Driscoll. 1988. The Role of the Recirculation Vortex in Improving Fuel-air Mixing within Swirling Flames. *Proc. 22nd Symposium (International) on Combustion*. The Combustion Institute, Pittsburgh. 531–54.
[9] H.S. Al-Kabie. 1989. *Radial Swirlers for Low Emissions Gas Turbine Combustion*. University of Leeds, Dept. of Fuel & Energy: PhD Theses.
[10] J. M. Beer and N. A. Chigier. 1972. *Combustion Aerodynamics*. Applied Science Publisher, London.
[11] FLUENT 14.0 2012. *User's Guide*. Fluent Inc.
[12] Y.M. Kim, and T.J. Chung. 1989. Finite- Element Analysis of Turbulent Diffusion Flames. *AIAA J*. 27(3): 330–339.
[13] K.R. Menzies. 2005. An Evolution of Turbulence Models for the Isothermal Flow in a Gas Turbine Combustion System. *Proc. 6th International Symposium on Engineering Turbulence Modelling and Experiments*, Sardinia, Italy.
[14] J.L. Da Palma. 1988. *Mixing in Non-Reacting Gas Turbine Combustor Flows*. PhD Thesis, University of London.
[15] F. Durst and D. Wennerberg. 1981. Numerical Aspects of Calculation of Confined Swirling Flows with Internal Recirculation. *Int. J. Numerical Methods Fluids*. 12: 203–224.
[16] W. Zhou, D. Moyeda, R. Payne and M. Berg. 2009. Application of numerical simulation and full scale testing for modelling low NOx burner emissions. *Combustion Theory and Modelling*. 13(6: 1053–1070.
[17] H.K. Versteeg and W. Malalasakera. 1995. *An Introduction to Computational Fluid Dynamics, the Finite Volume Method*. Longman Group Ltd.
[18] M.N. Mohd Jaafar, Y.A. Eldrainy and M.F. Ahmad. 2009. Investigation of Radial Swirler Effect on Flow Pattern inside Gas Turbine Combustor. *Modern Applied. Science* 3(5): 21-30.
[19] A.E. Yehia, S.A. Hossam M.S. Khalid and M.N. Mohd Jaafar. 2010. A Multiple. Inlet Swirler for Gas Turbine Combustors, *Int. J. Mechanical Syst. Sci. Eng.* 2(2): 106–109.
[20] M. N. Mohd Jaafar, M.S.A. Ishak and S. Saharin. 2010. Removal of NOx and CO from a Burner System. *Environmental Science and Technology*. 44 (8): 3111–3115